Design, Fabrication and Soundness Test of A Bi2223 Magnet Designed for Cooling by Liquid Hydrogen

Design, Fabrication and Soundness Test of A Bi2223 Magnet Designed for Cooling by Liquid Hydrogen

S. Imagawa, *IEEE member*, A. Iwamoto, S. Hamaguchi, Y. Shirai, *IEEE member*, R. Kawasaki, H. Ohya, F. Matsumoto, M. Shiotsu, M. Tsuda, Y. Nagasaki, T. Yagai, and H. Kobayashi

***Abstract*—The critical heat flux in liquid hydrogen is ten times higher than that in liquid helium and is approximately half of that in liquid nitrogen. Since the resistivity of pure metal such as copper or silver at 20 K is less than one-hundredth of that at 300 K, HTS magnets immersed in liquid hydrogen are expected to satisfy the fully cyostable condition or to be stable against high resistive heat generation enough for quench detection at a practical current density. In order to examine cryostability of HTS magnets in liquid hydrogen, a pool-cooled Bi2223 magnet with a 5 T magnetic field at 20 K has been designed, fabricated and tested in liquid nitrogen prior to excitation tests in liquid hydrogen. The magnet consists of six outer double pancake coils with the inner diameter of 0.20 m and four inner double pancake coils with the outer diameter of 0.16 m. The resistive voltage to initiate thermal runaway in the coil assembly in liquid nitrogen was higher than 1 V that is sufficient high for quench detection.**

***Index Terms*—Bi2223, liquid hydrogen, liquid nitrogen, pool-cooled, thermal runaway**

I. Introduction

QUENCH protection is crucial for HTS magnets because of slow propagation of a normal zone. Height of resistive voltage to initiate thermal runaway should be an important index for quench detection of HTS magnets to prevent the failure [1], [2]. The critical heat flux in liquid hydrogen is ten times higher than that in liquid helium and is approximately half of that in liquid nitrogen. Since the resistivity of pure metal such as copper or silver at 20 K is less than one-hundredth of that at 300 K, HTS magnets immersed in liquid hydrogen are expected to satisfy the fully cyostable condition or to be stable against high resistive heat generation enough for quench detection at a practical current density for electric power equipment. In order to examine cryostability of HTS magnets in liquid hydrogen toward establishment of the design method, a pool-cooled Bi2223 magnet with a 5 T magnetic field at 20 K has been designed and fabricated. A Bi2223 tape conductor, DI-BSCCO type H with width of 4.3 mm and height of 0.23 mm [3], was selected because cryostability of Bi2223 tapes stabilized with Ag is expected to be better than ReBCO tapes with high I_c. The magnet consists of six outer double pancake coils and four inner double pancake coils. Each double pancake coil has been tested in liquid nitrogen to check the soundness before assembling, and the whole assembly was tested in liquid nitrogen to evaluate the critical current, I_c, and the allowable heat generation, over which thermal runaway occurs, that is, the resistive voltage continues to rise.

The excitation tests in liquid hydrogen are planned at the end of 2021. Comparison of cryostability in liquid nitrogen and in liquid hydrogen is important to develop a prediction method of the allowable resistive voltage in liquid hydrogen from that in liquid nitrogen. This paper intends to summarize the design, fabrication, and test results in liquid nitrogen.

Manuscript received November 28, 2021. This work was funded by MEXT Grant #19H02130 and partly supported by NIFS Collaboration Research program (NIFS20KOBA032). *(Corresponding author: Shinsaku Imagawa.)*

S. Imagawa, A. Iwamoto and S. Hamaguchi are with the National Institute for Fusion Science, Toki, Gifu 509-5292, Japan (e-mail: imagawa@nifs.ac.jp, iwamoto@nifs.ac.jp, hamaguchi.shinji@nifs.ac.jp).

Y. Shirai, R. Kawasaki, H. Ohya, F. Matsumoto, and M. Shiotsu are with Kyoto University, Kyoto 606-8501, Japan (e-mail: shirai@energy.kyoto-u.ac.jp, kawasaki.rikako.54v@st.kyoto-u.ac.jp, oya.hikaru.46r@st.kyoto-u.ac.jp, matsumoto.fumiya.76c@st.kyoto-u.ac.jp, shiotsu@pe.energy.kyoto-u.ac.jp).

M. Tsuda, Y. Nagasaki are with Touhoku University, Sendai, Miyagi 980-8579, Japan (e-mail: tsuda@ecei.tohoku.ac.jp, nagasaki@ecei.tohoku.ac.jp).

T. Yagai is with Sophia University, Tokyo 102-8554, Japan (e-mail: tsuyoshi-yagai@sophia.ac.jp).

H. Kobayashi is with JAXA, Sagamihara, Kanagawa 252-5210, Japan (Email: kobayashi.hiroaki@jaxa.jp).

Color versions of one or more of the figures in this paper are available online at http://ieeexplore.ieee.org.

Digital Object Identifier will be inserted here upon acceptance.

II. Design of Magnet

A. Critical current of Bi2223

Critical field, B_k, of Bi2223 at temperature, T, is given by

$$B_k = b(1-T/T_c)(1-X(T)+((1+X(T))^2-4\nu_p X(T))^{0.5})/(1-\nu_p) \quad (1)$$

where $X(T) = a/(1-T/T_c)$. The critical temperature, T_c, is 108.4 K, and the numerical parameters a, b and ν_p are 0.65, 0.799 and 0.995, respectively [4], [5]. Since I_c of a Bi2223 tape conductor depends on the magnetic field normal to the tape plane [6], the parallel component is ignored for estimation of I_c in this paper. I_c of Bi2223 tapes at external magnetic field normal to the tape, B, can be fitted by

$$I_c = A(1-T/T_c)^p/B^q\,(1-B/B_k)^{r(T)} \quad (2)$$

where A, p, q and $r(T)$ are determined to fit the measured data. In the case of DI-BSCCO type H with I_c over 200 A at 77 K that is reported in [3], A = 644 A, p = 0.86, q = 0.15 and $r(T)$ = -1.53+0.218 T+0.004652 T^2-0.0001371 T^3 for T < 45 K. A = 986 A, p = 1.85, q = 0.2 and r (T) = 40.12-1.499 T+0.01999 T^2-8.649e-5 T^3 for T > 45 K. The fitting curves are shown in Fig. 1 in comparison with the measured data.

B. Concept of magnet design

In order to use the existing liquid hydrogen cryostat and experiment system in Noshiro Rocket Testing Center of JAXA (Japan Aerospace Exploration Agency) [7], the outer diameter of the 5 T magnet must be shorter than 0.27 m. A test sample area is prepared for coil-shaped conductor samples. Therefore, the magnet consists of a set of outer coils, named Coil-A, and a set of inner coils, named Coil-B, as shown in Fig. 2. The direction of current of Coil-B is opposite to that of Coil-A in order to enlarge the field at the sample area with decreasing the magnetic energy. A double pancake type is selected to avoid joints at the high field side. The coils with high I_c are installed at the high horizontal field area where are the top and bottom.

The inner diameter of Coil-A and the outer diameter of Coil-B are fixed at 0.20 m and 0.16 m, respectively, and parameters studies have been carried out. The major cases are listed in Table 1 where B_0 and W_B are the magnetic field at the center of the sample area and the magnetic energy. Finally, Case 2 was selected because of high B_0 and low W_B. The magnet consists of six outer double pancake coils and four inner double pancake coils. The turn numbers are 77 turns per layer for Coil-A and 73 turns per layer for Coil-B, and 4.7–4.9 T magnetic field is induced between Coil-A and Coil-B at the current of 400 A, as shown in Fig. 3. The load lines of the magnetic field normal to the tape are shown in Fig. 1.

C. Fabrication of magnet

The Bi2223 tapes are wrapped with one half overlap of Kapton tapes with the thickness of 0.0125 mm. The terminal of each double pancake coil is jointed to a copper block with solder. The terminals of Coil-A and Coil-B are located at the outer side and the inner side, respectively, as shown in Fig. 4a. Bobbins for winding were removed to enlarge the wetted area.

After the tests in liquid nitrogen, all the double pancake coils were assembled and supported by a set of stainless-steel plates, as shown in Fig. 4b. The copper blocks were clamped tightly with bolts. A gap of 0.2 mm for cooling is secured between the coils with Normex sheets and Kapton tapes. The fraction of contacting area, where is not wetted, between coils were around 30% at the first assembling. The contacting area is enlarged to around 50% before 4th cool-down of the coil assembly to reduce the compressive stress between the pancake coils induced by electromagnetic force.

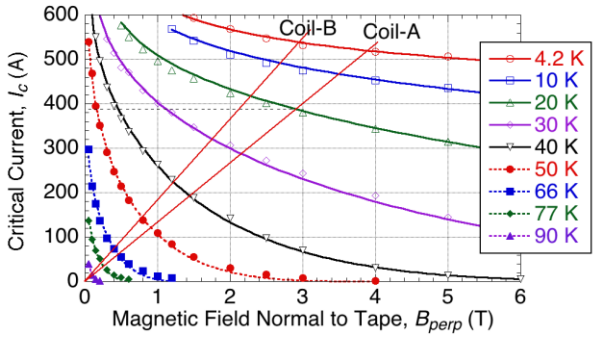

Fig. 1. Critical current of DI-BSCCO type H conductors versus magnetic field normal to the tape and load lines of the 5 T magnet. The symbols are measured data in [5], and lines are fitting curve by (2).

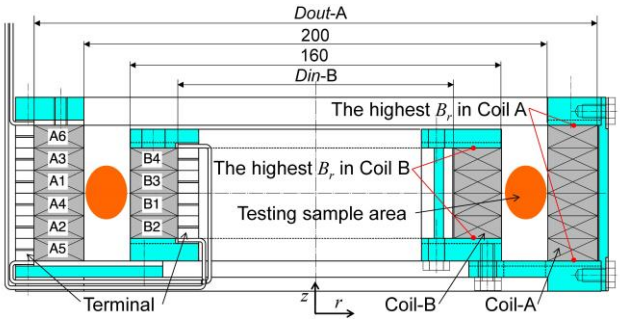

Fig. 2. Sketch of LH_2 cooled 5 T coil with Bi2223 tape conductors.

TABLE 1
PARAMETER STUDY OF COIL-A AND COIL-B AT 400 A

Case	Coil-A (m×n)	D_{out}-A (m)	Coil-B (m×n)	D_{in}-B (m)	B_0 (T)	W_B (kJ)	Length (m)
1	77×12	0.243	54×12	0.126	4.60	15.9	935
2	**77×12**	**0.243**	**73×8**	**0.119**	**4.70**	**16.8**	**899**
3	77×12	0.243	91×6	0.109	4.63	17.6	874
4	88×10	0.249	70×8	0.121	4.65	17.0	868

(Remarks) m and n are turn and layer numbers of Bi2223 tapes, respectively.

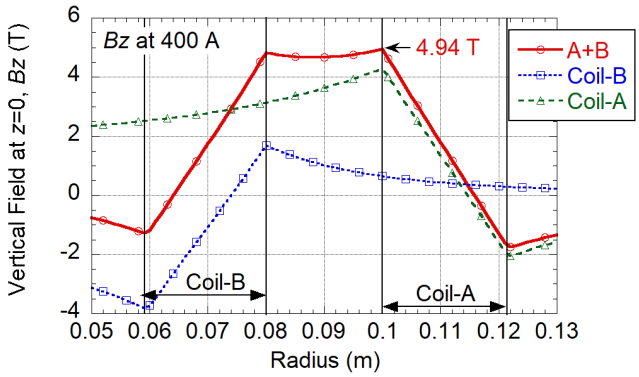

Fig. 3. Vertical magnetic field in the Case 2 in Table 1.

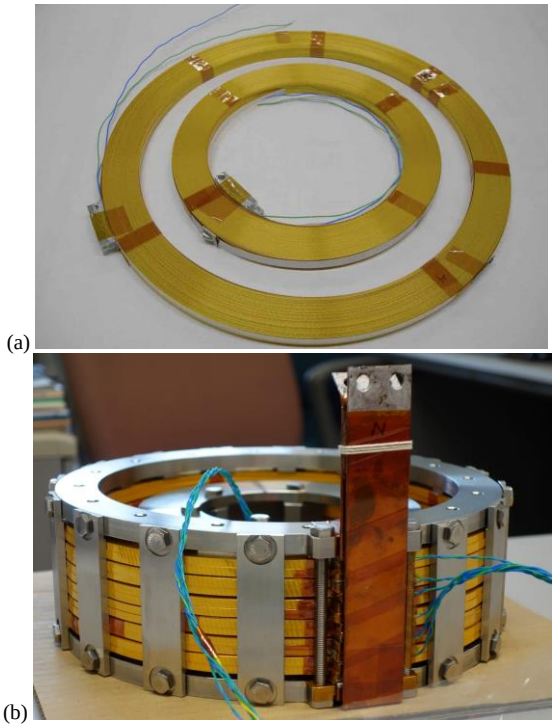

(a) (b)

Fig. 4. Photos of double pancake coils of Coil-A and Coil-B before tests in liquid nitrogen (a) and the coil assembly (b).

III. Test in Liquid Nitrogen

A. Double pancake coil

I_c and the voltage to initiate thermal runaway, V_{th}, were measured in liquid nitrogen. The wetted area fraction of each coil is around 90% in this test. In the I_c measurement, the current is ramped up and down to the voltage around 0.3 V by 0.2 A/s. The results of the double pancake coils are shown in Figs. 5a and 5b, where the inductive voltage is subtracted. I_c and n-value are estimated from the following equation:

$$V/L = E_0 (I/I_c)^n + a\, I \qquad (3)$$

where V, L, I and a are the terminal voltage, whole length of conductor, current and resistive component, respectively. E_0 is set at 0.1 mV/m.

I_c of each coil is consistent with I_c of each tape. Since the resistive component of A1-A6 coil is less than 10μΩ/m, degradation caused by winding process should be negligible. Apparent resistive parts were induced in B1, B2 and B3 coils. The degraded parts should be local because I_c and n-value seem not to be degraded. The degraded parts will be near the terminals because of the difficulty of soldering process of the terminals inside the coils.

Thermal runaway tests have been carried out for 8 coils after the I_c measurement. The current is ramped up by 1 A with holding for 30 or 60 s. When the coil voltage increases continuously, the current is dumped to an external resistor. The results are summarized in Table 2. Thermal runaway occurs at around 1.5 times higher current than I_c. A representative behavior of the voltage is shown in Fig. 6a, and the voltage of B3 coil, V_{th} of which is the lowest, is shown in Fig. 6b. Since the heat generation to initiate thermal runaway, Q_{th}, of B3 coil is clearly lower than the other coils, the heat generation should be concentrated. The V_{th} of B3 coil is, however, higher than 0.4 V which is sufficient high for quench detection.

Except for B3 coil, Q_{th} of Coil-B is around 80 W, which is 60% of that of Coil-A. The ratio is close to the ratio of wetted surface area. Anyway, Q_{th} is much lower than the maximum heat flux of the total wetted area. In the experiments, the transition to film boiling didn't occur before and after the thermal runaway and discharge of the current. The increase rate of heat generation against temperature rise should be higher than that of cooling under nucleate boiling.

B. Coil assembly

The double pancake coils with high I_c (A5, A6, B2, B4) are installed at top and bottom where the field is highest. Figure 7 shows the voltage of each double pancake coil in the coil assembly during excitation by 0.2 A/s up to 65 A in liquid nitrogen. I_c of each double pancake coil depends on the magnetic field, and the order and the values are consistent with I_c of the tapes. The lowest I_c is 42.2 A of A6 coil. The coil assembly can be excited without thermal runaway up to 65 A that is 1.5 times higher than I_c of A6 coil.

As shown in Figs. 8a and 8b, thermal runaway of the coil assembly occurred at 95 W (68 A, 1.4 V of A5 coil) in the 3rd cool-down and at 72 W (65 A, 1.1 V of A6 coil) in 4th cool-down, where the wetted area fraction was reduced from 70% to 50% for reduction of compressive stress between coils. Q_{th} seems proportional to the wetted area. Compared with the results of the double pancake coils, Q_{th} of A5 coil was lowered from 130 W to 95 W, which is reasonable because the wetted area fraction is reduced from around 90% to 70% and because the cooling channel is narrowed.

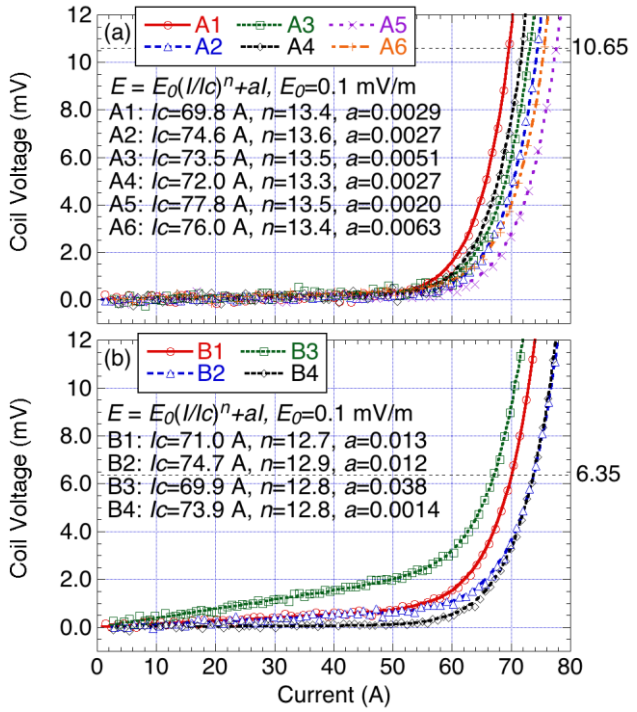

Fig. 5. Coil voltage of A1 to A6 coils (a) and B1 to B4 coils (b) during excitation in liquid nitrogen. I_c of each double pancake coil is estimated from 0.1 mV/m using the whole length of the conductor.

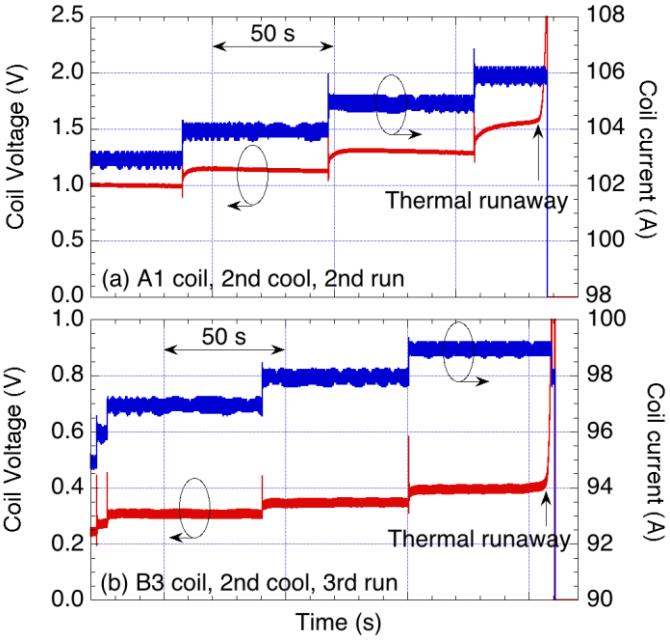

Fig. 6. Coil voltage and current of A1 coil (a), B3 coil (b) during step change of the current in liquid nitrogen. The wetted area fraction of each coil is around 90% in this test.

TABLE 2
CRITICAL CURRENT AND THE CURRENT TO INITIATE THERMAL RUNAWAY

Coil	I_c of tape (A)	I_c of DP (A)	Current (Heat generation) to initiate thermal runaway
A1	183	69.8	106 A (163 W)
A2	191	74.6	not measured
A3	193	73.5	107 A (121 W)
A4	197	72.0	107 A (145 W)
A5	211	77.8	113 A (130 W)
A6	207	76.0	not measured
B1	193	71.0	105 A (71 W)
B2	202	74.7	110 A (79 W)
B3	182	69.9	99 A (39 W)
B4	200	73.9	111 A (85 W)

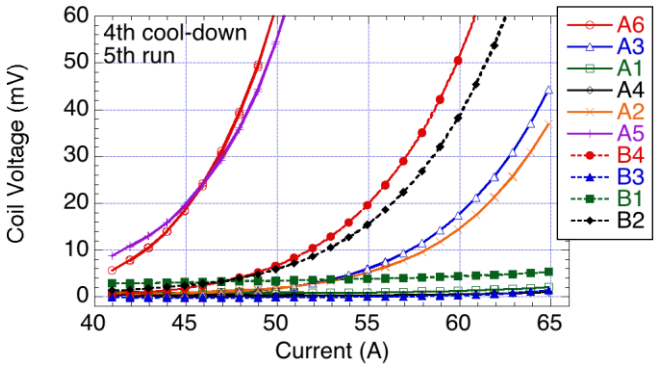

Fig. 7. Voltage of each double pancake coils in the coil assembly during excitation by 0.2 A/s up to 65 A in liquid nitrogen.

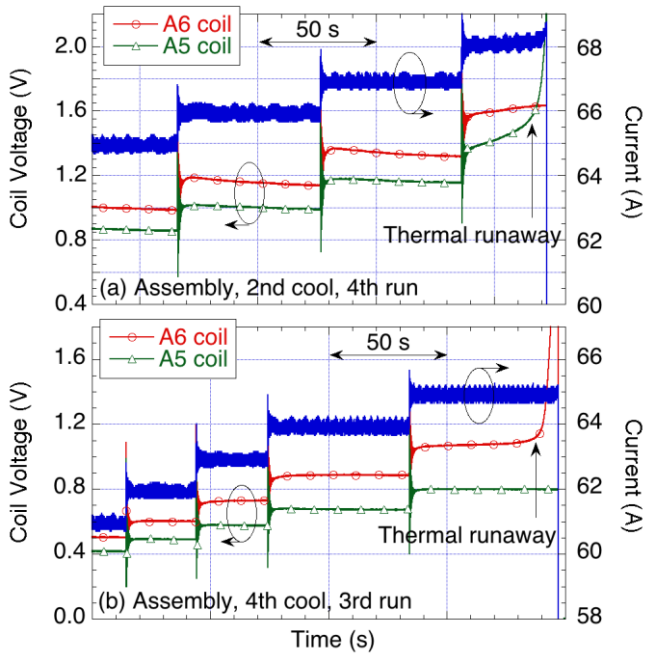

Fig. 8. Coil voltage of the coil assembly during step change of the current in liquid nitrogen in the 2nd coo-down (a) and 4th cool-down (b). The wetted area fraction was reduced from around 70% to 50% before the 4th cool-down.

IV. DISCUSSION

Heat balance of one conductor is considered assuming uniformity in the longitudinal direction. The electric field, E, of a Bi2223 tape conductor is given by

$$E = \min(E_0\,(I/I_c(B,\,T))^n,\; R_{Ag}(I\text{-}I_c(B,\,T))) \qquad (4)$$

where R_{Ag} is the resistance per unit length of the conductor. Ag ratio of this conductor is 1.8, and RRR is 15 [8]. The heat generation is given by $I\times E$. The heat flux of nucleate boiling in liquid nitrogen is given by $q = 0.039\Delta T^{2.5}$ (W/cm^2) for $\Delta T <$ 12 K where ΔT is temperature rise of the cooled surface [9]. The temperature of the Bi2223 can be calculated by adding ΔT and temperature rise in the Kapton tape and the Bi2223 tape.

Figure 9 shows a calculated result for Coil-A. The cooling power is multiplied by 2 with considering the heat removal by thermal conduction to the neighbor conductors. n-value of 5 is adopted to fit the measured flux-flow voltage at the high current region. Since the temperature dependence of heat generation in Bi2223 tapes is stronger than $\Delta T^{2.5}$, thermal runaway can occur under nucleate boiling region. Cryostable condition can be satisfied by increase of the wetted area fraction or by reduction of current density.

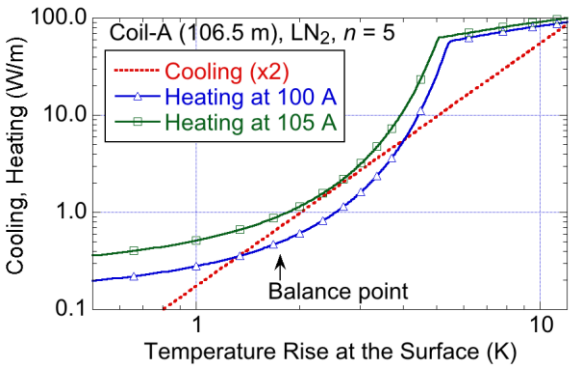

Fig. 9. Heat generation in the Bi2223 tape in Coil-A and cooling by nucleate boiling in liquid nitrogen. Thermal runaway occurs at 105 A because the heating is higher than the cooling in all range of temperature rise.

V. CONCLUSION

In order to examine cryostability of HTS magnets, a pool-cooled Bi2223 magnet with a 5 T magnetic field at 20 K has been designed, fabricated and tested in liquid nitrogen. As the results of tests for the double pancake coils and the coil assembly, thermal runaway in liquid nitrogen occurs at around 1.5 times higher current than I_c, and the heat generation to initiate thermal runaway seems proportional to the wetted area. The voltage to initiate thermal runaway in the coil assembly is higher than 1 V that is sufficient high for quench detection but is much lower than the maximum heat flux of the total wetted area in liquid nitrogen. Thermal runaway should occur under nucleate boiling region because the temperature dependence of heat generation in Bi2223 tapes is stronger than that of the heat flux in nucleate boiling region.

REFERENCES

[1] Fedor Gömöry and J´an Šouc, "Stability of DC transport in HTS conductor with local critical current reduction," *Supercond. Sci. Technol.*, vol. 34, 2021, Art. no. 025005.

[2] Y. Yanagisawa, E. Okuyama, H. Nakagome, T. Takematsu, T. Takao, M. Hamada, S. Matsumoto, T. Kiyoshi, A. Takizawa, M. Takahashi, and H. Maeda, "The mechanism of thermal runaway due to continuous local disturbances in the YBCO-coated conductor coil winding," *Supercond. Sci. Technol.*, vol. 25, 2012, Art. no. 075014.

[3] N. Ayai, T. Kato, J. Fujikami, S. Kobayashi, M. Kikuchi, K. Yamazaki, S. Yamade, T. Ishida, K. Tatamidani, K. Hayashi, K. Sato, R. Hata, H. Kitaguchi, H. Kumakura, K. Osamura and J. Shimoyama, "DI-BSCCO Wire with Ic over 200 A at 77 K", *Journal of Physics: Conference Series*, vol. 97, 2008, Art. no. 012112.

[4] T. Kiss, S. Nishimura, M. Inoue, H. Okamoto, M. Kanazawa, and Y. Sumiyoshi, "E-J characteristics of Bi-2223/Ag tapes as a function of temperature, magnetic field and angle", *Advances in Cryogenic Engineering*, vol. 48B, 2002, 1091-1101.

[5] T. Kiss, M. Inoue, T. Kuga, M. Ishimaru, S. Egashira, S. Irie, T. Ohta, K. Imamura, M. Yasunaga, M. Takeo, T. Matsushita, Y. Iijima, K. Kakimoto, T. Saitoh, S. Awaji, K. Watanabe, and Y. Shiohara, "Critical current properties in HTS tapes," *Physica C*, vol. 392–396, 2003, 1053–1062.

[6] P. Sunwong, J. S. Higgins, and D. P. Hampshire, "Angular, temperature, and strain dependencies of the critical current of DI-BSCCO tapes in high magnetic fields," *IEEE Trans. Appl. Supercond.*, vol. 21, no. 3, June 2011, 2840-2844.

[7] Y. Shirai, M. Shiotsu, H. Tatsumoto, H. Kobayashi, Y. Naruo, S. Nonaka, Y. Inatani, "Critical current test of liquid hydrogen cooled HTC superconductors under external magnetic field," *Physics Procedia*, vol. 81, 2016, 158–161.

[8] T. Naito, H. Fujishiro, and Y. Yamada, "Thermal conductivity of single and multi-stacked DI-BSCCO tapes," *Cryogenics*, vol. 49, 2009, 429–432.

[9] E. G. Brentari and R. V. Smith, "Nucleate and film pool boiling design correlations for O2, N2, H2, and He," *Advances in Cryogenic Engineering*, vol. 10, 1965, 325–341.